

Spin-relaxation process of holes in type-II $\text{Al}_{0.34}\text{Ga}_{0.66}\text{As}/\text{AlAs}$ multiple quantum wells

Tadashi Kawazoe, Yasuaki Masumoto, and Tomobumi Mishina
Institute of Physics, University of Tsukuba, Tsukuba, Ibaraki 305, Japan
 (Received 24 August 1992)

We have measured the spin memory and the spin-relaxation times of holes in type-II quantum wells by means of pump-and-probe methods. The fast Γ - X interlayer scattering which is characteristic of type-II multiple quantum wells allows us to observe directly the hole spin-relaxation process. The hole spin relaxation is described by two decay components. The faster decay time ranges from 20 to 100 ps and depends on the number density of "antiparallel-spin" holes. This indicates that the scattering between up-spin holes and down-spin holes is the major spin-relaxation process of holes. The slower time component is about 20 ns, which is probably ascribed to the spin relaxation of localized holes in the well layers.

The spin-relaxation process of carriers in semiconductors has been extensively studied by means of static luminescence polarization measurements. Such measurements have informed us of spin-relaxation mechanisms of carriers in bulk semiconductors.¹ Today, ultrafast laser spectroscopy is used to observe directly the time-resolved polarization.²⁻¹⁰ Recently the time-resolved polarization measurement is often applied to GaAs quantum wells.^{2-4,7-10} In quantum wells, two-dimensionality splits the degenerate valence bands into heavy- and light-hole bands whose total angular momenta are $\frac{3}{2}$ and $\frac{1}{2}$, respectively. As a result of the nondegeneracy, spin-relaxation processes of holes in quantum wells are quite different from those in bulk crystals and are studied intensively.^{11,12}

Time-resolved luminescence polarization experiments were done in type-II as well as type-I GaAs quantum wells. Kohl *et al.* observed that the electron spin-relaxation time is 150 ps in good quality type-I GaAs/ $\text{Al}_x\text{Ga}_{1-x}\text{As}$ quantum wells at 10 K.⁷ In short-period type-II GaAs/AlAs quantum wells, van der Poel *et al.* reported that hole spin memory remains longer than the lifetime of carriers, 7 μs , at 1.7 K.^{2,3} The polarized luminescence comes from the radiative recombination of spin-polarized electrons and holes. Therefore, it is not clear which are polarized, electrons or holes. To overcome this difficulty, Damen *et al.* measured the spin-relaxation time of electrons and holes individually by using *p*- and *n*-doped GaAs/ $\text{Al}_{0.3}\text{Ga}_{0.7}\text{As}$ type-I multiple quantum wells.⁹ The obtained spin-relaxation times of electrons and holes are 150 and 4 ps, respectively. The pump-and-probe technique is also applied to the time-resolved studies of spin relaxation of electrons and holes. Bar-Ad and Bar-Joseph measured the spin relaxation of carriers in the GaAs/ $\text{Al}_x\text{Ga}_{1-x}\text{As}$ type-I quantum wells.¹⁰ They observed two decay times, 120 and 50 ps. They ascribed 120 ps to the spin-relaxation time of electrons and 50 ps to that of holes.

We measured the spin-relaxation processes of holes in type-II $\text{Al}_{0.34}\text{Ga}_{0.66}\text{As}/\text{AlAs}$ multiple quantum wells by means of the pump-and-probe method. In a type-II sample, photogenerated electrons are quickly scattered to the

barriers, so that holes alone remain in the wells.¹³⁻¹⁷ The pump-and-probe method is applicable to the observation of hole states. In fact, the experimental results give unique information about the hole spin relaxation. We can observe how to relax the spin polarization of the nondegenerate holes in this two-dimensional system in detail. The hole spin-relaxation time ranges from 20 to 100 ps, depending on the excitation intensity. We also observed that 10% spin memory is still conserved for an order of a nanosecond.

We can observe directly the spin relaxation of holes in type-II quantum-well structures. Figure 1(a) shows the electronic energy levels of the $\text{Al}_{0.34}\text{Ga}_{0.66}\text{As}/\text{AlAs}$ type-II quantum-well structures. Both the bottom of the con-

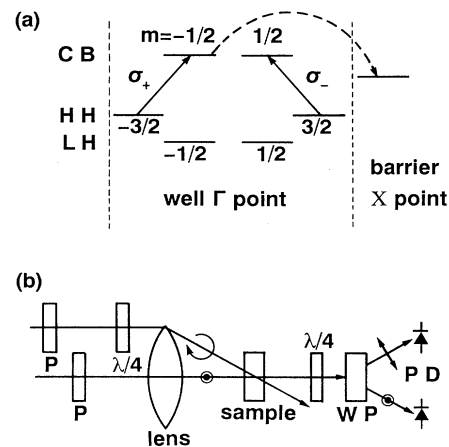


FIG. 1. (a) Optical transitions and interlayer electron transfer for type-II $\text{Al}_{0.34}\text{Ga}_{0.66}\text{As}/\text{AlAs}$ quantum wells with circularly polarized light. σ_+ and σ_- stand for right and left circularly polarized light, respectively. Electrons at Γ points in wells transfer to the X points in barriers. As a result, holes alone remain in the wells. (b) Experimental setup of the pump-and-probe method: P, polarizer; $\lambda/4$, quarter-wave plate; WP, Wollaston prism; PD, photodiode. Arrows denote polarization of light.

duction and the top of the valence band in the $\text{Al}_{0.34}\text{Ga}_{0.66}\text{As}$ well are at the Γ point in the Brillouin zone. The Γ -point bottom of the conduction band is linked to the X point in the AlAs barrier by the interlayer intervalley scattering of electrons. σ_+ and σ_- denote right circularly polarized light and left circularly polarized light, respectively. The arrows in Fig. 1(a) indicate the allowed transitions induced by σ_+ and σ_- .

When the right circularly polarized light hits the heavy-hole absorption edge, the electrons at the $-\frac{1}{2}$ state and the holes at the $-\frac{3}{2}$ state are generated. As a result of the Γ - X interlayer scattering, Γ electrons whose spin angular momentum is $-\frac{1}{2}$ are scattered to the X point in the barriers. The mean scattering time is less than a few picoseconds.¹³ After electrons at the $-\frac{1}{2}$ state are scattered to the X point in barriers, holes at the $-\frac{3}{2}$ state alone are left in the well. Therefore, we can measure the spin relaxation of holes by observing the hole density at the states $-\frac{3}{2}$ and $\frac{3}{2}$ which are probed by right and left circularly polarized light, respectively.

Figure 1(b) shows the experimental setup. A quarter-wave plate transforms the linearly polarized pump beam into circularly polarized light. The probe beam is the linearly polarized light which is the sum of an equal amount of right circularly polarized light and left circularly polarized light. The probe beam transmitted through the sample goes through another quarter-wave plate. The right circularly polarized light component turns to the vertically linearly polarized light and the left circularly polarized light to the horizontally linearly polarized light. Two linearly polarized lights are separated by a Wollaston prism and are detected by two photodiodes whose sensitivities are equal to each other. The obtained signals, I_+ and I_- , are proportional to the differential transmittance of the right and the left circularly polarized light, respectively. Namely, I_+ is proportional to the hole density at the $-\frac{3}{2}$ state and I_- is proportional to that at the $\frac{3}{2}$ state. In addition, a simple differential electronic circuit is used to obtain the signal $I_+ - I_-$ corresponding to the spin polarization. In this way, we can take very weak spin memory signals that are not usually detectable. A detectable degree of polarization is as small as 0.1%. The advantage of this method comes from the cancellation of the temporal fluctuations of laser power, because I_+ and I_- are measured simultaneously.

The sample used in this investigation is 100 periods of 9.2-nm $\text{Al}_{0.34}\text{Ga}_{0.66}\text{As}$ and 2.7-nm AlAs layers which form type-II ternary alloy multiple-quantum-well structures. A fundamental optical characterization of the sample and its ultrafast laser spectroscopy were reported in our previous publications.^{13,17,18} The sample was directly immersed in superfluid helium and was measured at 2 K. We used the same cavity-dumped synchronously pumped dye laser system that was used in our previous study.¹⁸⁻²⁰ The temporal width of laser pulses was 1 ps. The repetition rate was varied to be 406 kHz, 812 kHz, and 4.06 MHz.

Figure 2 shows an experimental result. The excitation density is $0.07 \mu\text{J}/\text{cm}^2$ corresponding to the sheet carrier

density of $2.1 \times 10^9/\text{cm}^2$. The laser repetition rate is 812 kHz. The inset shows the excitation photon energy and the absorption spectrum of the sample, indicating that the excitation photon energy corresponds to the absorption edge of the heavy-hole exciton. Both I_+ and I_- signals show a sharp structure at the beginning. The initial sharp structure in the I_- signal is ascribed to the coherent artifact. The initial sharp structure in the I_+ signal is the exciton bleaching plus the coherent artifact. As a result of interlayer intervalley scattering of electrons, exciton bleaching decays at a time constant of 2.5 ps and hole bleaching remains for a long time. After 10 ps, I_- decreases slowly, while I_+ increases at almost the same rate. This means that the holes created at the state $-\frac{3}{2}$ relax to the state $\frac{3}{2}$. Even after 1 μs , the I_+ signal is not zero but is equal to I_- . Because the hole lifetime in this sample is an order of a microsecond,¹⁸ and because the pulse-to-pulse interval is 1.2 μs , the absorption bleaching still remains at the negative time delay. The result shows that the spin memory is completely lost in μs , while the holes still remained in the wells. This means that the hole lifetime is much longer than the spin-relaxation time.

Figure 2(b) shows the logarithmic plot of $I_+ - I_-$. We can consider that $I_+ - I_-$ is proportional to degree of polarization because the relaxation time of $I_+ + I_-$ is of μs order. After 10 ps, the signal decays exponentially at a time constant of 67 ps. At this time region, there are

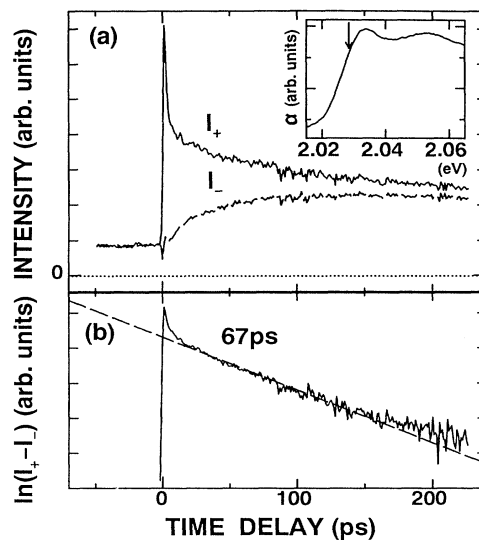


FIG. 2. (a) The differential transmission signals observed under the pump of the right circularly polarized light. The pump density is $0.07 \mu\text{J}/\text{cm}^2$. The laser repetition rate is 812 kHz. The solid line shows the differential transmission signal of the right circularly polarized probe light. The dashed line shows the differential transmission signal of the left circularly polarized probe light. The inset shows the absorption spectrum of the $\text{Al}_{0.34}\text{Ga}_{0.66}\text{As}/\text{AlAs}$ multiple quantum wells with arrowed excitation photon energy. (b) The logarithmic plot of $I_+ - I_-$. The decay of $I_+ - I_-$ is fitted by single exponential decay (dashed line).

no electrons in the well as a result of the Γ - X interlayer scattering. Therefore, the time constant of 67 ps means the spin-relaxation time of holes. Furthermore, we observed the dependence of the relaxation time of holes on the excitation density.

The hole spin-relaxation time depends upon the excitation density and ranges from 20 to 100 ps. Figure 3 shows the temporal change of $I_+ - I_-$ at three excitation densities. The relaxation time becomes shorter with an increase in excitation density. The hole spin-relaxation time becomes faster as the excitation density increases. We also measured $I_+ - I_-$ for the long-time scale. We observed that a 10% spin memory is still conserved for an order of a nanosecond. The results show that spin relaxation has another slow decay time component whose time constant is about 20 ns. Similar slow decay is observed in the Γ - X luminescence of short-period type-II GaAs/AlAs quantum wells by van der Poel *et al.*^{2,3}

The fast decay component depends not only on the excitation density but also on the repetition rate of the laser pulses. In a previous work, we clarified that the lifetime of holes in the well layer is as long as an order of a microsecond in a type-II $\text{Al}_{0.34}\text{Ga}_{0.66}\text{As}/\text{AlAs}$ sample.¹⁸ The long lifetime of holes forms a base signal at the negative time delay in the temporal trace of the pump-and-probe experiment, which is proportional to the number density of accumulated holes. When the right circularly polarized light hits the heavy-hole absorption edge, the electrons at the $-\frac{1}{2}$ state and the holes at the $-\frac{3}{2}$ state are generated. After the photoexcitation, generated holes coexist with holes generated by the previous pulses, because the inverse of the repetition rate of the laser is comparable to the lifetime of holes. Holes generated by the previous pulses lose the spin memory completely and half of them are at the $\frac{3}{2}$ state. We call the holes at the $\frac{3}{2}$ state "antiparallel-spin" holes. We also call the holes at the $-\frac{3}{2}$ state "parallel-spin" holes.

We plotted the spin-relaxation rate of holes as a function of number density of antiparallel-spin holes. The number density of antiparallel-spin holes is proportional to the bleaching signal taken by left circularly polarized

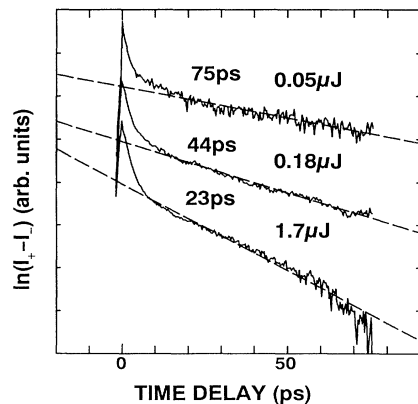


FIG. 3. The logarithmic plot of $I_+ - I_-$ for three excitation densities. Three decay curves of $I_+ - I_-$ are fitted by single exponential decay (dashed lines).

light. Differential transmittance of 1% due to the bleaching of the hole state corresponds to the hole number density of $2.2 \times 10^9/\text{cm}^2$ which is calibrated at the excitation density of $0.1 \mu\text{J}/\text{cm}^2$. Therefore, the number densities of antiparallel-spin holes are obtained from the bleaching signal of I_- at 10 ps. The result is shown in Fig. 4. Data include the results taken at three different repetition rates, 406 kHz, 812 kHz, and 4.06 MHz. Changing the repetition rate corresponds to changing the equal number densities of "parallel-spin" holes and "antiparallel-spin" holes, while changing the excitation density corresponds to changing mainly the number density of parallel-spin holes.

The relation is well written by a straight line, that is, $1/\tau = A + BN$, where $1/\tau$ is the spin-relaxation rate, A is 0.0054 ps^{-1} , B is $0.084 \times 10^{-10} \text{ ps}^{-1} \text{ cm}^2$, and N is the sheet number density of antiparallel-spin holes. The spin-relaxation rate of holes is proportional to the number density of holes which have an opposite spin. Another plot of the spin-relaxation rate of holes as a function of total number density of holes gives the scattering of data. The experimental result definitely shows that the hole-hole collision dominates the spin-relaxation mechanism of holes and that up-spin holes selectively collide with down-spin holes.

Collisions of two identical particles are discussed in quantum mechanics.²¹ The identity of the particles leads to the symmetric or antisymmetric orbital wave function of the system, according to whether their spins are antiparallel or parallel to each other. The scattering cross section of two holes are represented by $d\sigma_s = |f(\theta) + f(\pi - \theta)|^2 d\theta$, when the spins of the holes are antiparallel to each other. Here, $f(\theta)$ is a part of the outgoing wave function $f(\theta)e^{ikr}/r$ from the scattering center, and $d\theta$ is an element of the solid angle. On the

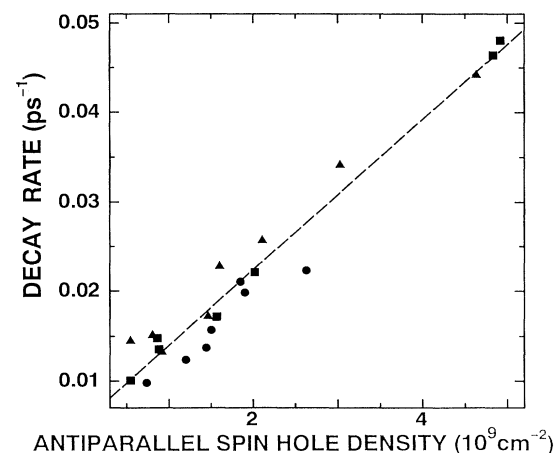


FIG. 4. The plot of the hole spin-relaxation rate as a function of the "antiparallel-spin" hole density. A dashed line is the fitted line $1/\tau = A + BN$; N is a sheet number density of "antiparallel-spin" hole, A is 0.0054 ps^{-1} , and B is $0.084 \times 10^{-10} \text{ ps}^{-1} \text{ cm}^2$. The solid squares, solid triangles, and solid circles correspond to the data taken at the repetition rates of 406 kHz, 812 kHz, and 4.06 MHz, respectively.

other hand, the scattering cross section of two holes is described by $d\sigma_a = |f(\theta) - f(\pi - \theta)|^2 d\theta$, when the spins of the holes are parallel to each other. The two-dimensional Coulomb scattering cross section is analytically obtained.²² However, we cannot find that $d\sigma_s$ is much larger than $d\sigma_a$.²³ If hole wave vector is small compared with the radius of action of the scattering potential, $f(\theta)$ is constant.²¹ This situation corresponds to the scattering of rigid spheres. Then, $d\sigma_a$ is zero, but $d\sigma_s$ is finite. This means that antiparallel-spin holes are scattered to each other, but that parallel-spin holes are not scattered to each other. The two-dimensional screened Coulomb potential is proportional to $1/r^3$ and the condition of slow particle scattering can be satisfied in this case.^{21,24} Therefore, the two-dimensional screened Coulomb scattering may explain the reason why antiparallel-spin holes are mutually scattered much more than parallel-spin holes. Further theoretical investigation is needed to explain the experimental results.

In III-V semiconductors, valence-hole states are characterized by mixture of orbital angular momentum of $j = 1$ and spin angular momentum of $s = \frac{1}{2}$. In quantum wells, subband mixing takes place further. As a result, spin is not the good quantum number. Therefore,

change in the wave vector of holes caused by hole scattering brings about the change in the spin state.^{11,12} In the slower time domain, holes are considered to be localized at the interface fluctuation. Holes scarcely collide with each other. The spin-relaxation time then becomes slower. We think localization of holes is responsible for this slow spin-relaxation time of 20 ns.

In summary, we measured the spin-relaxation time of holes in type-II $\text{Al}_{0.66}\text{Ga}_{0.34}\text{As}/\text{AlAs}$ multiple quantum wells by means of the pump-and-probe technique. Spin relaxation of holes is described by fast and slow relaxation rates. The fast spin-relaxation time of holes ranges from 20 to 100 ps and depends on the antiparallel-spin hole density. The fast spin relaxation of holes is caused by hole-hole collision. The slow spin-relaxation time of holes is about 20 ns. Slow spin relaxation is probably ascribed to the localization of holes.

This work was supported by a Scientific Research Grant-in-Aid No. 04228202 for Scientific Research on a Priority Area—Ultrafast and Ultraparallel Optoelectronics—by the Ministry of Education, Science and Culture of Japan.

¹Optical Orientation, edited by F. Meier and B. P. Zakharchenya (North Holland, Amsterdam, 1984).

²W. A. J. A. van der Poel, A. L. G. J. Severens, H. W. van Kesteren, and C. T. Foxon, Phys. Rev. B **39**, 8552 (1989).

³W. A. J. A. van der Poel, A. L. G. J. Severens, H. W. van Kesteren, and C. T. Foxon, Superlatt. Microstruct. **5**, 115 (1989).

⁴A. Tackeuchi, S. Muto, T. Inata, and T. Fujii, Appl. Phys. Lett. **56**, 2213 (1990).

⁵M. R. Freeman, D. D. Awschalom, J. M. Hong, and L. L. Chang, Phys. Rev. Lett. **64**, 2430 (1990).

⁶M. R. Freeman and D. D. Awschalom, J. Appl. Phys. **67**, 5102 (1990).

⁷M. Kohl, M. R. Freeman, D. D. Awschalom, and J. M. Hong, Phys. Rev. B **44**, 5923 (1991).

⁸T. C. Damen, Karl Leo, Jagdeep Shah, and J. E. Cunningham, Appl. Phys. Lett. **58**, 1902 (1991).

⁹T. C. Damen, Luis Viña, J. E. Cunningham, Jagdeep Shah, and L. J. Sham, Phys. Rev. Lett. **67**, 3432 (1991).

¹⁰S. Bar-Ad and I. Bar-Joseph, Phys. Rev. Lett. **68**, 349 (1992).

¹¹T. Uenoyama and L. J. Sham, Phys. Rev. Lett. **64**, 3070 (1990).

¹²T. Uenoyama and L. J. Sham, Phys. Rev. B **42**, 7114 (1990).

¹³Y. Masumoto, T. Mishina, F. Sasaki, and M. Adachi, Phys. Rev. B **40**, 8581 (1989).

¹⁴J. Feldmann, R. Sattmann, E. O. Göbel, J. Kuhl, J. Hebling, K. Ploog, R. Muralidharan, P. Dawson, and C. T. Foxon,

Phys. Rev. Lett. **62**, 1892 (1989).

¹⁵J. Feldmann, J. Nunnenkamp, G. Peter, E. Göbel, J. Kuhl, K. Ploog, P. Dawson, and C. T. Foxon, Phys. Rev. B **42**, 5809 (1990).

¹⁶P. Saeta, J. F. Federici, R. J. Fischer, B. I. Greene, L. Pfeiffer, R. C. Spitzer, and B. A. Wilson, Appl. Phys. Lett. **54**, 1681 (1989).

¹⁷Y. Masumoto and T. Tsuchiya, J. Phys. Soc. Jpn. **57**, 4403 (1988).

¹⁸T. Mishina, F. Sasaki, and Y. Masumoto, J. Phys. Soc. Jpn. **59**, 2635 (1990).

¹⁹T. Mishina and Y. Masumoto, Phys. Rev. B **44**, 5664 (1991).

²⁰T. Mishina and Y. Masumoto, Jpn. J. Appl. Phys. **31**, L343 (1992).

²¹L. D. Landau and E. M. Lifshitz, *Quantum Mechanics (Non-relativistic Theory)* (Pergamon, Oxford, 1977).

²²F. Stern and W. E. Howard, Phys. Rev. **163**, 816 (1967).

²³Two-dimensional Coulomb scattering cross section for identical holes is derived as $\sigma_s = (G/2k)\tanh(\pi G)(1/\sin^2(\theta/2) + 1/\cos^2(\theta/2) + \cos\{2G \ln[\tan(\theta/2)]\}/\sin(\theta/2)\cos(\theta/2))$ and $\sigma_a = (G/2k)\tanh(\pi G)(1/\sin^2(\theta/2) + 1/\cos^2(\theta/2) - \cos\{2G \ln[\tan(\theta/2)]\}/\sin(\theta/2)\cos(\theta/2))$, where G is defined by $1/a^*k$. Here a^* is the effective Bohr radius and k is the wave vector of holes.

²⁴T. Ando, A. B. Fowler, and F. Stern, Rev. Mod. Phys. **54**, 437 (1982).